RSC Advances

PAPER

View Article Online
View Journal | View Issue

Cite this: *RSC Adv.*, 2025, **15**, 48628

Synthesis and application of a deep eutectic solvent as a green catalyst for use in oil esterification: DOE optimization and method greenness analysis

Sassi Siddiqui,[a] Mahabash Khanzada,[a] Saima Qayoom Memon, *[a] Amber Rehana Solangi [b] and Muhammad Yar Khuhawar[a]

Deep eutectic solvents (DESs), as a new generation of green solvents, have attracted the attention of researchers because they meet all the requirements of green chemistry. DESs are made by combining a hydrogen-bond acceptor (HBA) and a hydrogen-bond donor (HBD) in a solid-phase reaction and are liquids at room temperature with melting points lower than those of the individual components. In the current research, new DESs containing tetrabutylammonium bromide as hydrogen-bond acceptor (HBA) and oxalic acid as a hydrogen-bond donor (HBD) in mole ratios of 1 : 1 to 1 : 5 have been synthesized and characterized by FT-IR and NMR spectroscopy. The physicochemical properties and electrochemical behavior of the DES have also been investigated. Cytotoxic studies on 3T3 cell lines showed no toxic effects of the synthesized DES. It showed no inhibition of 5 different microorganisms, confirming its eco-friendly, non-toxic and biocompatible nature. The synthesized DES was used as a green catalyst in place of sulphuric acid for the esterification of used oil. The esterification efficiency was optimized using the design of experiment (DoE) approach by varying the amounts of methanol and DES and the reflux time. An esterification efficiency of 96.3% was achieved at optimum variable values of 8.5 mL methanol, 0.5 g DES and 10 min reflux time at 60 °C. Analysis of variance showed that the amount of DES was the most significant variable. The effects of interaction variables, *i.e.*, DES amount with reflux time and methanol volume with reflux time, were also found to be statistically significant. The greenness indices of the classical esterification reaction and the DES-based esterification were compared using three different greenness methods, namely, the National Environmental Methods Index (NEMI), the Analytical Procedure Index (GAPI) and the Analytical Eco-Scale method. A comparative method greenness analysis of the catalysts reported for the esterification reaction was conducted using the Analytical Eco-Scale method.

Received 29th August 2025
Accepted 17th November 2025

DOI: 10.1039/d5ra06461a

rsc.li/rsc-advances

1 Introduction

The unique properties of ionic liquids (ILs), such as low volatility,[1] low melting point,[1] high thermal stability, wide range of solubility and non-flammability, have been a topic of interest in research. However, the synthesis of ILs involves the use of halogenated compounds and imidazolium salts, which contradicts the idea of green analytical chemistry (GAC); furthermore, their preparation is energy-intensive, and the final products usually require organic solvents for purification. In light of these challenges, researchers are increasingly focusing on deep eutectic solvents (DESs), a category of solvents that have applications in almost every field of science and share many of the properties and features of ILs. DESs are composed of two or more solid components that give a mixture with a lower melting point than the starting materials;[2] however, because the components are connected by a hydrogen-bond network, they are structurally different from ionic liquids. The first synthesized DES was reported by Abbott,[3] and DESs have since been replacing ionic liquids for many applications.[4] So far, most of the studies have been focused on eco-friendly, biodegradable and green solvents based on choline chloride, a quaternary ammonium salt.[5–9] Recently, tetrabutylammonium bromide (TBAB), a quaternary ammonium salt, has emerged as a phase transfer catalyst for a variety of organic transformations.[10,11] The physical properties of various synthesized DES have been reported.[7,8,12–15] This paper explores the synthesis of DESs based on TBAB with different ratios of oxalic acid, in contrast to the literature, where mainly equimolar amounts of HBA and HBD have been reported. Based on the physicochemical and electrochemical analysis, the best DES was identified and used as a catalyst for esterification reactions. Esters are among the most essential compounds in organic chemistry, with applications in various industrially significant products. The key factors for industrial applications

[a]*DrM.A.Kazi Institute of Chemistry, University of Sindh, Jamshoro, Pakistan. E-mail: saimaqmemon@usindh.edu.pk*

[b]*National Center of Excellence in Analytical Chemistry, University of Sindh, Jamshoro, Pakistan*

aimed at enhancing reaction rates are the activity, stability and reusability of the catalyst. Common catalysts used in esterification are homogeneous catalysts, such as sulphuric acid, and heterogeneous catalysts, such as ion exchange resins, ionic solvents and some deep eutectic solvents.[16] Sulphuric acid is a good catalyst used in classical esterification reaction; *i.e.*, the Fischer process. However, sulphuric acid is considered hazardous because of its corrosive properties. In contrast to sulphuric acid and ionic liquids, deep eutectic solvents offer a low-cost and biodegradable alternative.[4] In order to make informed decisions for the adoption of DES as a green alternative, it is important to evaluate the environmental sustainability through the use of greenness index analysis of esterification reactions using DES as a catalyst. Factors such as energy consumption, solvent toxicity and waste generation can be evaluated using the National Environmental Methods Index (NEMI),[17] the Green Analytical Procedure Index (GAPI)[18] and the Analytical Eco-Scale method.[19]

The National Environmental Methods Index (NEMI) tool provides a quick view of a method's environmental friendliness. It uses the criteria of pH, the hazardous nature of generated waste, and bioaccumulation. The Green Analytical Procedure Index is a more comprehensive evaluation procedure that considers the entire analytical procedure. Green, yellow and red colors in the generated pictogram highlight the environmental impact of each step of a reaction. A semi-quantitative tool based on the penalty points for toxicity, energy consumption and waste generated for an analytical method is called the Analytical Eco-Scale. A higher score on the Analytical Eco-Scale indicates a greener method.

2 Experimental methods

2.1 Synthesis and toxicity measurement of DESs

DES was synthesized by mixing tetrabutylammonium bromide as a hydrogen-bond acceptor and oxalic acid as a hydrogen-bond donor by following the reported method.[20] DESs were synthesized in different molar ratios, *i.e.*, 1 : 1, 1 : 2, 1 : 3, 1 : 4, and 1 : 5, with constant stirring at 300 rpm at 80 °C for 2–3 hours until homogeneous, transparent, pale-yellow and viscous solutions were obtained. All the synthesized DESs were stored in sealed laboratory vials and kept in a desiccator over silica gel and used without further treatment.

The toxic effects of DES were evaluated on the 3T3 cell line using American Type Culture Collection (ATCC) CRL-1658 lot no. 59049195. Cells were cultured in Dulbecco's Modified Eagle Medium, supplemented with 5% fetal bovine serum (FBS), 100 IU mL^{-1} penicillin, and 100 μg mL^{-1} streptomycin in 75 cm^2 flasks and kept in a 5% CO_2 incubator at 37 °C. The extent of MTT reduction to formazan within the cells was calculated at different time intervals by measuring the absorbance at 540 nm using a microplate reader (Spectra Max plus, Molecular Devices, CA, USA). The cytotoxicity was recorded as the concentration causing 50% growth inhibition (IC_{50}) for 3T3 cells. The percent inhibition was calculated by using the following formula:

$$\%\ \text{Inhibition} = 100 - ((\text{mean of O.D. of test compound} - \text{mean of O.D. of negative control})/(\text{mean of O.D. of positive control} - \text{mean of O.D. of negative control}) \times 100).$$

2.2 Characterization of synthesized DESs

The synthesized DESs were characterized by FT-IR and ^{1}H NMR spectroscopic techniques. FT-IR spectra for DESs of different mole ratios and pure oxalic acid and TBAB were also recorded with a Thermo-Nicolet FT-IR spectrometer equipped with a diamond ATR accessory. The proton NMR spectrum of 1 : 4 DES was taken in DMSO in order to further confirm the structure of the synthesized DES.

The viscosities and densities of all the DESs were measured using a viscometer and an R.D. bottle.

2.3 Electrochemical behavior of the synthesized DES

The electrochemical measurements were conducted on a CHI760 electrochemical workstation (USA) with a single-compartment, three-electrode system. A GC electrode was used as the working electrode and Pt as the counter electrode. HCl (0.1 M) was taken as a bare electrolyte, and the synthesized DESs were scanned as reported in the previous work.[21] The experiments were performed at room temperature, and a potential window of +1.5 ± 0.4 mV was selected for CV scans.

Conductivity measurements of the synthesized DES were performed at room temperature (30 °C) with a conductivity meter (Orion 150Aplus). The cell values were periodically checked by using solutions of known conductivity.

2.4 Experimental setup for esterification reaction

The influence of the process parameters on the esterification reaction, as well as the optimum conditions with respect to percent yield, was investigated using a multifactorial design of experiments approach with three factors, analyzed using StatGraphics® Centurion XVI software. Prior to use, low-quality, used semi solid oil was heated at 70 °C until a uniform phase was formed. For the esterification reaction, 1 g of liquid oil was placed in a closed jacket reactor with an overhead condenser. Different volumes of DES catalyst (0.5–3.5 wt%) and methanol (5 mL–20 mL) were added to the reactor. The reaction mixture was heated for 10–120 min while stirring continuously at 350 rpm. All the experimental runs were performed thrice to ensure accuracy. The FFA content was calculated as the weight percentage of acid produced during the reaction, based on the modified AOCS official method Ca-5a-40.[22] For the titrimetric analysis, 1.0 g of the oil sample was dissolved in 50 mL of isopropanol and 0.1% phenolphthalein solution was added as an indicator. The solution was then titrated with 0.1 N potassium hydroxide until a persistent faint pink color appeared. The product yield, which indicated the conversion of (free fatty acid) FFA into free fatty acid methyl ester (FAME), was calculated using the following equation;

$$\text{Conversion} = \frac{\text{FFA}_i - \text{FFA}_0}{\text{FFA}_i}$$

Table 1 The matrix of experiments for factorial design and the responses recorded as percent yield

	Parameters			Results
Run	Volume of methanol (mL)	Amount of DES (g)	Reflux time (min)	Efficiency (%)
1	5.00	3.50	65.00	0.00
2	12.50	3.50	120.00	75.00
3	5.00	2.00	120.00	0.00
4	5.00	2.00	10.00	0.00
5	12.50	0.50	10.00	80.00
6	12.50	2.00	65.00	24.00
7	20.00	3.50	65.00	46.00
8	12.50	3.50	10.00	24.50
9	20.00	2.00	120.00	20.00
10	20.00	2.00	10.00	5.00
11	12.50	0.50	120.00	68.00
12	12.50	2.00	65.00	23.50
13	12.50	2.00	65.00	23.50
14	5.00	0.50	65.00	80.00
15	20.00	0.50	65.00	48.00

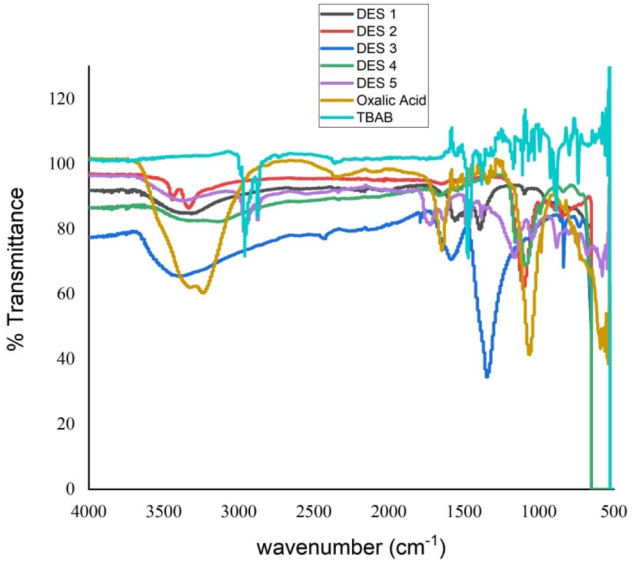

Fig. 1 FT-IR spectra of DESs at different mole ratios of TBAB to oxalic acid.

where FFA_i and FFA_0 are the initial and final values of free fatty acids before and after esterification, respectively.

Esterification reactions using sulphuric acid were also conducted for comparison. Table 1 shows the conditions under which 15 experimental runs were conducted, and the % efficiency of the esterification for each experiment is also reported.

2.5 Recovery of DES after esterification

In order to evaluate the reusability of the DES as a catalyst, recovery tests were performed. For this purpose, after esterification, the reaction mixture was centrifuged at 3000 rpm for about 15 min. The methanol and oil separated into two layers due to their difference in viscosity and density. The methanol layer was evaporated and the oil layer was centrifuged again at 3000 rpm for 10 min, which separated the DES. The FT-IR of the recovered DES was recorded in order to confirm the structure.

2.6 Cytotoxic and microbial investigation of DES

Cytotoxicity tests were conducted to determine whether the DES exhibited harmful effects on cell viability and growth function.[23] For the cytotoxicity test, 3T3 cell lines were used with three different ratios of DES. The effect of the DES on the inhibition of microbial activity was also studied using the three different ratios.

3 Result and discussion

3.1 FT-IR and ^{1}H NMR spectroscopy

The formation of DESs based on TBAB and oxalic acid with different mole ratios was confirmed by studying the Fourier transform infra-red (FT-IR) spectra in the range of 4000 cm^{-1} to 500 cm^{-1} and the ^{1}H NMR spectra.

In Fig. 1, the IR spectra of pure compounds, *i.e.*, TBAB and oxalic acid, and mixtures of different mole ratios are presented. The spectra show the carbonyl stretching peak at 1733 cm^{-1}, and the C–H vibration peaks at 2959 cm^{-1} and 2874 cm^{-1} are attributed to the –COOH of oxalic acid. In pure oxalic acid, the O–H stretching vibration appears as a broad band around 3400 cm^{-1} for the O–H, which shifts towards 3350 cm^{-1} in 1 : 1 DES. The C–H stretching of the *n*-butyl group appears at 2910 cm^{-1}. A stretching vibrational band shift from 1644 cm^{-1} to 1695 cm^{-1} for the C=O group was observed in the DESs, showing the interaction of TBAB and oxalic acid. As the mole ratio of oxalic acid to TBAB increases, the broad O–H peak stretches and flattens, and a significant reduction in intensity can be seen, especially in 1 : 4 DES. These observations suggest the formation of strong hydrogen bonds. A high carbonyl stretching peak is observed at 1 : 3 and 1 : 4 ratios, and the C–N stretching peak shifts in the 1 : 4 DES. Different mole ratios were synthesized up to 1 : 10, but there were no significant differences; therefore, these are not reported here. This suggests that TBAB–OxA complexes in those ratios were likely to be solutions of TBAB in OxA.[24]

The ^{1}H NMR spectrum (Fig. 2) in DMSO shows the characteristic signals of tetrabutyl ammonium bromide; *i.e.* a triplet near 0.95–1.00 ppm of the terminal protons, a multiplet at around 1.25–1.34 ppm corresponding to the γ-methylene protons, and a signal at 1.55–1.65 ppm attributed to the β-methylene protons, which appear as a multiplet because of coupling with adjacent methylene protons. A broad triplet can be seen around 3.15–3.25 ppm corresponding to the α-methylene protons directly bonded to the quaternary ammonium nitrogen. The broadening in the NMR signal is attributed to the hydrogen bond interaction between the ammonium and oxalic acid moieties.

Based on the observed FT-IR spectra and supported by the NMR spectrum, the structure of the tetrabutyl ammonium bromide–oxalic acid deep eutectic solvent is proposed in Fig. 3.

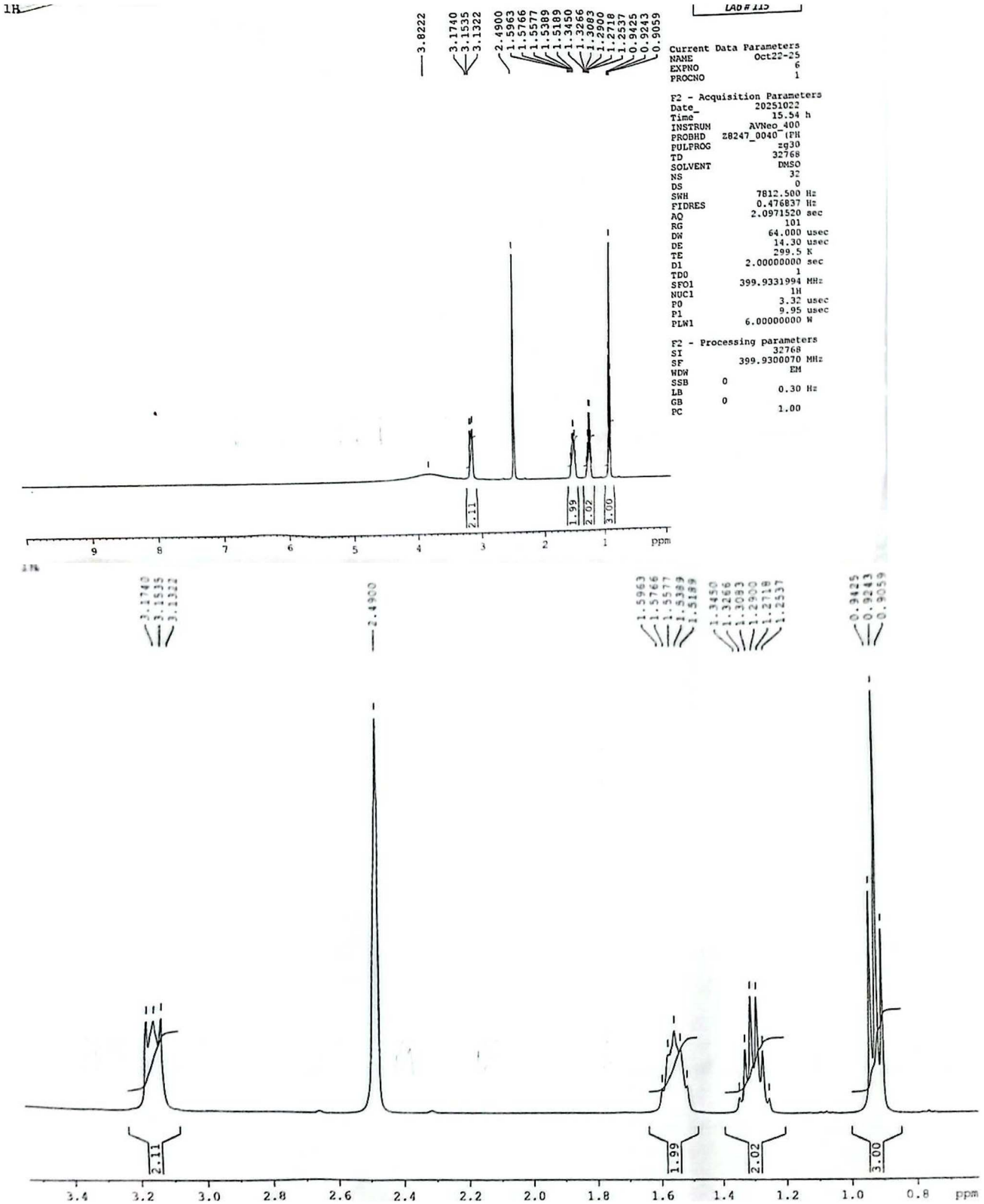

Fig. 2 ^{1}H NMR spectrum of 1 : 4 DES (top) and an expanded spectrum (bottom).

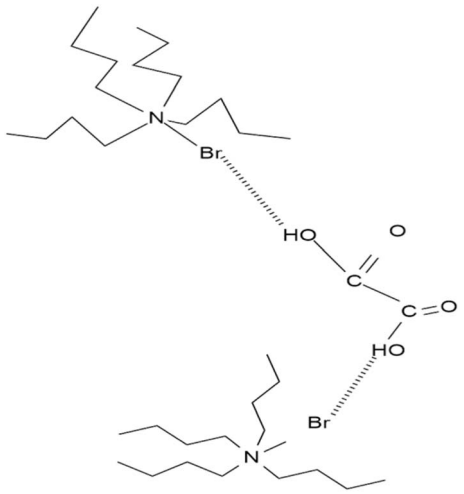

Fig. 3 Proposed structure of the deep eutectic solvent based on TBAB–oxalic acid.

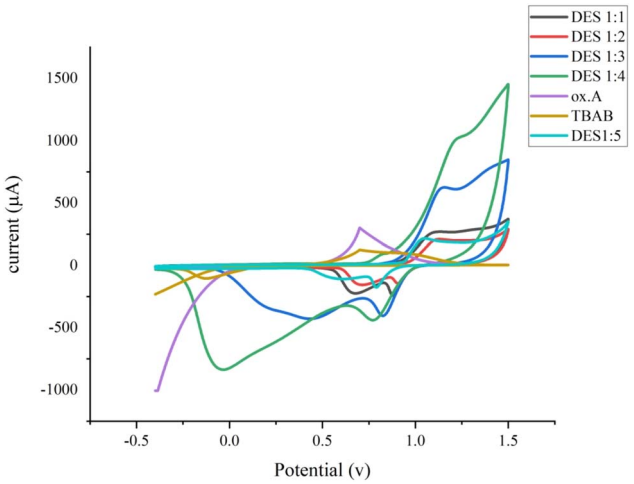

Fig. 4 Cyclic voltammograms of the DESs synthesized in 5 different mole ratios.

3.2 Electrochemical properties of DES

Cyclic voltammetry is one of the most common and powerful techniques for studying electrode reactions.[25] To investigate whether DES can replace costly ionic liquid (IL) electrolytes, CV scans were conducted.[26,27]

In order to investigate the redox behavior of the synthesized DES, a CV scan of each DES was taken. Fig. 4 shows cyclic voltammograms (CVs) of all 5 DESs. As can be seen from the figure, the shape of the curve and the peak positions of each DES vary. DES 1 : 4 shows the strongest redox current, suggesting enhanced electron transfer. TBAB and oxalic acid alone show very small redox peaks in comparison to those of the DESs, which have strong redox peaks. The order of DES activity with respect to their ratios is DES 1 : 4 > DES 1 : 3 > DES 1 : 2 > 1 : 1 and 1 : 5. DES 1 : 5 and 1 : 1 have the lowest redox response. The results suggest that the DES ratio significantly affects the electrochemical performance of the DES, and, in this case, DES 1 : 4 exhibited the optimum response.

This data also correlates with the conductance data. Table 2 shows that the conductivity increases with the increase in the amount of HBD from 1 : 1 to 1 : 4, then there is a slight decrease at 1 : 5. The highest conductance is at 1 : 4, *i.e.*, 9340 μS cm^{-1}, as is the current response. DES 1 : 5 shows a lower electrochemical response and a lower conductivity than DES 1 : 4. The higher conductivity improves ion mobility and reduces solution resistance, thereby facilitating the charge transfer reaction.

Table 2 Physicochemical properties of the synthesized deep eutectic solvent

DES (HBA : HBD)	Viscosity (mPa s)	Density (kg m^{-3})	Conductance (μs cm^{-1})
1 : 01	2.1502	1097.76	1203
1 : 02	2.1430	1016.78	1503
1 : 03	2.075	1018.87	3270
1 : 04	1.989	1020.96	9340
1 : 05	1.910	1042.80	6030

3.3 Conductivity, viscosity and density measurements of the synthesized DES

Table 2 shows the physicochemical properties of all 5 synthesized DESs. The increase in mole ratio of oxalic acid in the DES enhances the ionic conductivity and ion mobility, reduces the viscosity, and promotes faster diffusion of ions up to a mole ratio of 1 : 4; a drastic increase in conductance can be seen as the ratio increased from 1 : 3 to 1 : 4. Further, the conductivity decreases as the molar ratio of oxalic acid increases to 1 : 5, which can be explained on the basis of a saturation point, beyond which further additions of oxalic acid may not lead to more dissociation. The results are found to be comparable to those in the literature.[20]

Viscosity and density measurements were also carried out because these are important properties of a liquid for industrial applications. DESs are quite high in rank of viscosity and are lower in their conductivity as compared to ionic liquids and other solvents.[28] Table 2 shows the effect of increasing the amount of HBD on the viscosity of the DES. The viscosity of the DES decreases with increasing mole ratios, which may be due to the increase in the strength of the intermolecular interactions between TBAB–OxA and OxA–OxA. This trend is consistent with the findings of Zhao *et al.*,[29] who investigated choline acetate and glycerol. However, this contrasts with the studies by Sazali[30] and Abbot *et al.*,[31] who examined choline chloride and glycerol, where the viscosity only

Table 3 Toxicity of DES with different ratios

DES ratio	Cell line	Effect trend	IC_{50} ± SD
TBAB : oxalic acid 1 : 3	Cell 3T3	No effect	—
TBAB : oxalic acid 1 : 4	Cell 3T3	No effect	—
TBAB : oxalic acid 1 : 5	Cell 3T3	No effect	—

Table 4 Antimicrobial activity of three different DESs against five microbial organisms

DES ratio	Micro-organism	% Inhibition of compound	% Inhibition (ofloxacin)
TBAB : oxalic acid 1 : 3	*E. Coli*	No inhibition	95.27
TBAB : oxalic acid 1 : 3	*Bacillus subtillus*	No inhibition	96.83
TBAB : oxalic acid 1 : 3	*S. aureus*	No inhibition	94.40
TBAB : oxalic acid 1 : 3	*Pseudomonas aerogenosa*	No inhibition	95.07
TBAB : oxalic acid 1 : 3	*Ssalmonella typhi*	No inhibition	94.51
TBAB : oxalic acid 1 : 4	*E. Coli*	No inhibition	95.27
TBAB : oxalic acid 1 : 4	*Bacillus subtillus*	No inhibition	96.83
TBAB : oxalic acid 1 : 4	*S. aureus*	No inhibition	94.40
TBAB : oxalic acid 1 : 4	*Pseudomonas aerogenosa*	No inhibition	95.07
TBAB : oxalic acid 1 : 4	*Salmonella typhi*	No inhibition	94.51
TBAB : oxalic acid 1 : 5	*E. Coli*	No inhibition	95.27
TBAB : oxalic acid 1 : 5	*Bacillus subtillus*	No inhibition	96.83
TBAB : oxalic acid 1 : 5	*S. aureus*	No inhibition	94.40
TBAB : oxalic acid 1 : 5	*Pseudomonas aerogenosa*	No inhibition	95.07
TBAB : oxalic acid 1 : 5	*Salmonella typhi*	No inhibition	94.51

decreased with the addition of ChCl salt, which disrupts hydrogen bonding in the three-dimensional glycerol structure, thereby increasing the molecular freedom and decreasing the viscosity of the ChCl mixture. In contrast, no disruption was observed with TBAB and oxalic acid. This discrepancy is likely due to different effects that the type of salt has on the viscosity of the resulting mixture. A possible explanation for this could be that as the molar ratios of salt to hydrogen-bond donor (HBD) decrease, the salt may function as a bridge connecting the ionic groups. A lower salt concentration in the DES likely leads to a less dense network between the different groups, resulting in a decrease in viscosity.[32] The values are comparable to those in the literature.[20] A decrease in the density of DES with the increase in the mole ratio of HBD in DES could be due to the higher concentration of solute, which results in a tightly packed molecular arrangement.[24] The results are also found to be comparable to those in the literature.[20]

Table 5 Estimated results for esterification efficiency

	Experimental efficiency (%)	Efficiency predicted by model (%)
Row	Value	Value
1	0.0	3.31
2	75	68.4
3	0.0	3.31
4	0.0	−1.56
5	80	86.6
6	24	23.6
7	46	51.1
8	24.5	22.7
9	20	21.6
10	1.0	−2.31
11	68	69.8
12	23.5	23.7
13	23.5	23.7
14	80	74.9
15	48	44.7

3.4 Cytotoxicity and microbial activity inhibition

It is clear from electrochemical and conductance results that the best formed DES is obtained with a 1 : 4 ratio; therefore, the cytotoxic effects of three different DES, one below 1 : 4 and one above 1 : 4, were tested on the 3T3 cell line. No cytotoxic effects of the studied DESs were observed when the 3T3 cell line was treated with 100 μM DES (Table 3) as compared to the standard drug doxorubicin.

Table 4 shows that all three tested ratios of DES showed no inhibition for five different microbes. These results confirm that the synthesized DES are eco-friendly, non-toxic and biocompatible in nature, suggesting their suitability for microbial fuel cells or biosensor systems.

3.5 Use of DES as a catalyst in the esterification reaction

3.5.1 Esterification reaction optimization using DoE. The data obtained from 15 experiments were processed and fitted in a quadratic polynomial model using StatGraphic software. Table 5 shows the % efficiency values of esterification reactions obtained from 15 experiments and the predicted values by the model for the same experimental conditions. The R^2 (%) value

Table 6 Analysis of variance for % efficiency

Source	Mean square	*F*-ratio	*P*-value
A: methanol volume	153.125	3.940	0.104
B: amount of DES	2128.780	54.840	0.001
C: reflux time	413.281	10.650	0.022
AA	1249.500	32.190	0.002
AB	1521.000	39.180	0.001
AC	90.250	2.320	0.188
BB	5396.190	139.000	0.000
BC	976.563	25.160	0.004
CC	0.002	0.000	0.995
Total error	38.821		

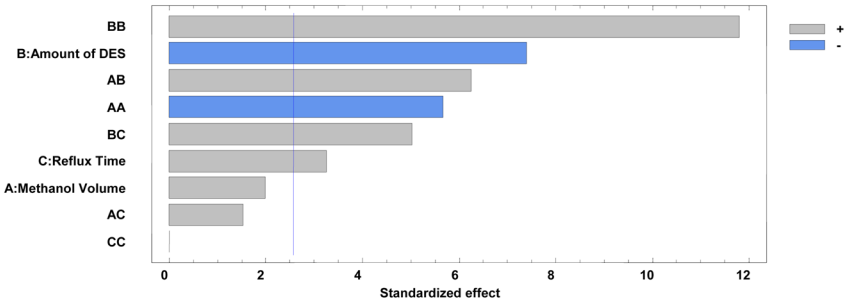

Fig. 5 Standardized Pareto chart for esterification yield.

Table 7 Optimum conditions for yield

Factor	Low	High	Optimum
Methanol volume (mL)	5.0	20.0	8.58
Amount of DES (g)	0.5	3.5	0.5
Reflux time (min)	10.0	120.0	10.0

between experimental and predicted values was found to be 98.45, showing the suitability of the used model.

3.5.2 Analysis of variance and Pareto chart. Table 6 shows the analysis of variance for the model used for optimization. The terms *A*, *B*, and *C* show the effect of the main variables, whereas *AB*, *AC*, *etc.* show the effect of the interaction of variables on % efficiency. The lower the value of *p* and the higher the value of *F*, the more significant is the effect of the variable on % efficiency.[33] Table 6 shows that the amount of DES is the most significant variable, based on the *p* and *F* values. The interactive effect of DES amount, reflux time, methanol volume, and reflux time was also found to be significant.

The same can be confirmed by the Pareto chart (Fig. 5), which also clarifies whether the effect of the variable is direct or indirect. All the variables and their interactive effects crossing the vertical line are considered to have a significant effect on the % efficiency of the esterification reaction; the + (grey) and − (blue) indicates whether the effect is direct or indirect, respectively. The amount of DES has a significantly positive effect on the percentage efficiency, which means that an increase in the amount of DES increases the percentage efficiency of the esterification.

3.5.3 Validation of the optimized reaction conditions. The predicted optimum conditions for achieving the highest yield are presented in Table 7; the predicted optimum yield by the model was 95.99% while the reflux temperature was fixed at 60 °C. The predicted optimum values were validated by conducting the esterification reaction at the predicted optimum values; the % efficiency obtained was 96.3%.

3.6 Comparison with previous work

In Table 8, the % esterification efficiency of the present work is compared with those of DESs reported previously for esterification reactions using different DESs.[34–37] The results show that the DES presented in this work is comparable in terms of efficiency and temperature, and better in terms of time.

3.7 Greenness index (analysis)

The green characteristics of the DES-based esterification were compared with those of the classical Fischer esterification reaction. Fischer's reaction uses concentrated sulphuric acid as the catalyst, while the sample to methanol ratio for the free fatty acid esterification is usually 10 : 1–20 : 1.[38]

Table 9 shows the percent efficiency of esterification reactions using sulphuric acid reported in the literature. It is clear from the table that the reactions use higher amounts of sulphuric acid, and the energy and time required for the reactions are also higher, making them less green. The greenness analyses of both sulphuric acid and DES-based reactions were therefore evaluated.

Three different greenness methods, namely, the National Environmental Methods Index (NEMI), the Analytical Procedure Index (GAPI), and the Analytical Eco-Scale were used for comparison of DES-based esterification reactions with that of the acid catalyst based reaction. It is worth mentioning that the comparison is made only for esterification reactions and not the catalyst synthesis; *i.e.*, DES *vs.* sulphuric synthesis.

3.7.1 NEMI method of greenness measurement. This approach involves a circle that is divided into four quadrants,

Table 8 Comparison of esterification efficiency of the DES

DES	% Efficiency (conditions)	Ref.
Ch.Cl : sorbitol	97 (180 °C for 180 min)	34
K_2CO_3 : glycerol 1 : 32.58	98 (60 °C for 68.58 min)	35
Ch.Cl : oxalic acid 1 : 1	40 (75 °C for 360–450 min)	36
Triphenylphosphoniumbromide : *p*-toluenesulfonic acid monohydrate	95 (150 °C for 30 min)	37
Oxalic acid : TBAB	96.3 (60 °C for 10 min)	Present work

Table 9 Reported esterification efficiencies using sulphuric acid as the catalyst

Reactants	Catalyst	% Yield (reaction conditions)	Ref.
2-Ethyl hexanol : nanoic A (5 : 1)	H_2SO_4 (1 mol%)	80% (70 °C,800 rpm, 120 min)	39
Oleic acid : oleyl alcohol (1 : 1)	H_2SO_4 (1.25%)	93% (90 °C, 300 min)	40
C. minutissima microbial oil : methanol (9 : 1)	H_2SO_4 (3%)	96% (80 °C, 480 min)	41
Tall oil fatty acid : methanol (15 : 1)	H_2SO_4 (0.5%)	96.7% (55 °C, 60 min)	42
Used oil : methanol (1 : 10)	H_2SO_4 (0.05%)	32% (60 °C, 30 min)	Present work

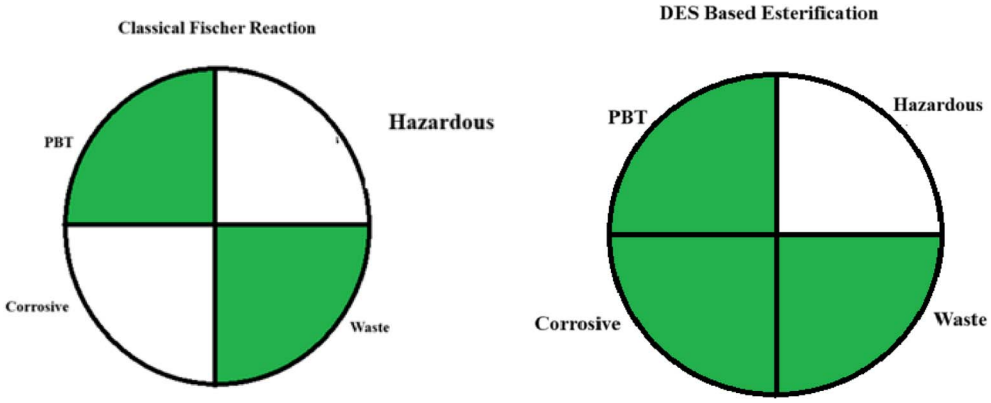

Fig. 6 Greenness of the Fischer and DES-based esterification reaction using the NEMI index.

each quadrant is green or white, based on Keith's classification.[17] The first quadrant is labeled as persistent, bioaccumulative and toxic (PBT), a method is less green if any chemical used is listed in the EPA's Toxic Release Inventory (TRI) chemicals list as a PBT.[43] The second quadrant is filled if a chemical used in the method is hazardous, as entered in the Federal Regulation list.[44] The third quadrant is designated as corrosive if the pH during the reaction is less than 2 or greater than 12. Finally, a method is less green if the amount of waste generated is >50 g.

Fig. 6 shows the greenness measurement of both reactions using the NEMI method, as per the TRI, methanol is considered as hazardous, which is common in both methods, however it is important to note that the amount of methanol used in the DES based method is less than that used in classical method, the DES-based method is therefore considered greener based on the NEMI index.

3.7.2 Green analytical procedure index (GAPI). The Green Analytical Procedure Index (GAPI) for the classical Fischer esterification reaction was compared to that of the DES-based esterification reaction. All five parameters, including sample collection, sample preparation, catalyst/solvent used during the reaction, instrument used, and hazards associated with the generated waste, were evaluated as described by J. Plotka *et al.*[18] GAPI uses a pentagram with three colors, *i.e.*, green, yellow and

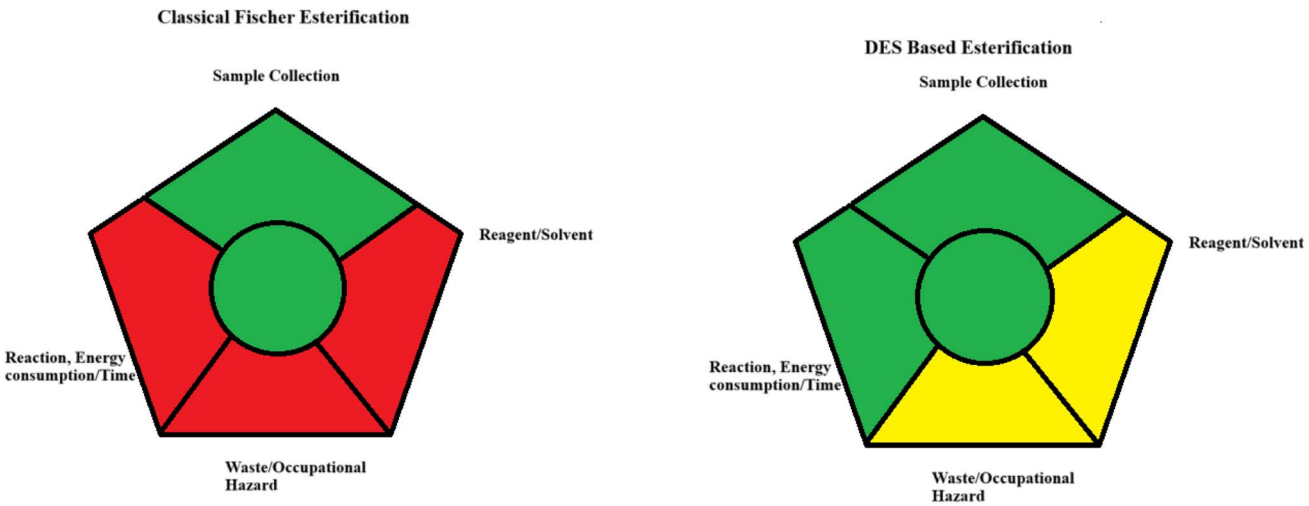

Fig. 7 GAPI greenness evaluation of the Fischer reaction and the DES-based esterification reaction.

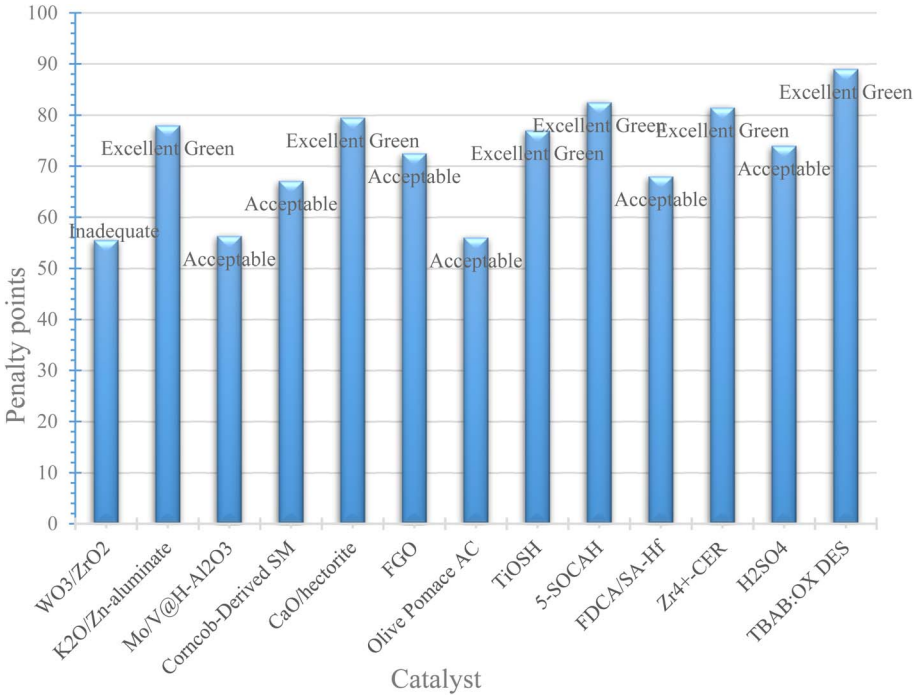

Fig. 8 Analytical eco-scale assessment of the esterification reaction using different catalysts.

red, to quantify low, medium and high environmental impact of each step, respectively.

Fig. 7 classifies the greenness of the Fischer esterification and the reaction based on DES using GAPI. The circle in the pentagram shows the type of method used for analysis, *i.e.*, titration, in both the Fischer and DES-based esterification reactions.

The Fischer reaction uses both methanol and sulphuric acid, and requires a large amount of base to neutralize the reaction. In contrast, the DES-based method uses smaller amounts of methanol as well as a very small amount of DES. The final product in acid-catalyzed esterification usually requires large amounts of base for neutralization, which is not the case in the DES-based esterification. The reaction time for optimum esterification is much less in the DES-based reaction; hence, less energy is consumed.

3.7.3 Analytical eco-scale. Van-Akenet al.,[19] proposed an interesting approach named the eco-scale for green organic synthesis evaluation. In this method, an ideal reaction is assigned a score of 100 in the eco-scale, which uses inexpensive reactants and is conducted at room temperature with a 100% yield, and is safe for both the operator and the environment. Penalty points are deducted from the ideal score for each of the parameters that differ from "the ideal value". Based on the score, methods are considered as "Excellent Green" if the score is >75, "Acceptable Green" when the score is 50–75, and "Inadequate Green" for a score of <50. In case of the Fischer reaction, the total penalty points are 6 for methanol, 8 for concentrated sulphuric acid, 2 for reflux (*i.e.*, energy use), 6 for acidic waste, 2 for solvent amount, and 2 for occupational hazard, making a total of 26 penalty points.[45] The final eco-scale score of the method is thus 74, which falls in the range of acceptable. DES-catalyzed esterification has 11 penalty points and a total score of 89 (Fig. 8), which makes the method Excellent Green on the eco-scale. Along with sulphuric acid, 11 (ref. 46–55) other catalysts have been assessed for their greenness, and the results are shown in Fig. 8. As seen from the figure, the DES-based esterification has the minimum penalty points. Four methods among the 11 are considered Excellent Green, with a total score of more than 75 on the eco-scale, while one method, with less than 50 points, is found to be inadequate.

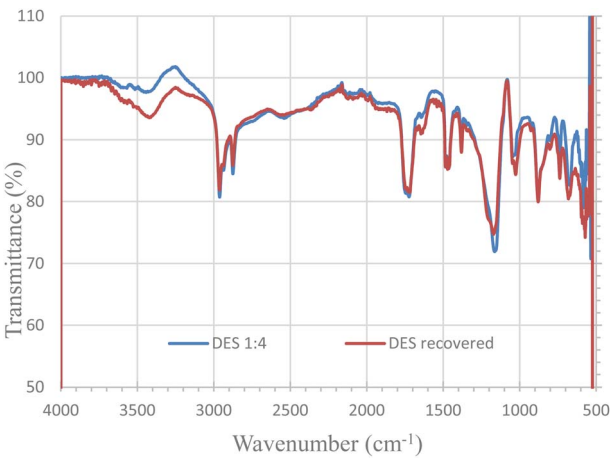

Fig. 9 Comparison of FT-IR spectra of DES before and after the esterification reaction.

3.8 Recovery of DES

After the esterification reaction, the DES was recovered by centrifugation. Fig. 9 shows the IR spectra of DES before esterification and the DES recovered after esterification. The IR spectra showed no major peak shifts, indicating the successful recovery of the DES.

4 Conclusion

The successful synthesis and characterization of DES with different mole ratios, along with insights into the physicochemical and electrochemical properties, are reported. It was observed that the viscosity, density and conductivity of the DESs mainly depend on the mole ratios of the HBD used to synthesize the DES. The non-inhibitory behavior of the DES towards microbes was observed, which highlights the potential of these solvents in applications where microbial viability is essential. For the first time, the electrochemical behavior of a DES based on TBAB and oxalic acid was studied, and the results indicate the different potential windows for each ratio of DES, with slight changes. Furthermore, the DES exhibits well-defined redox peaks, indicating electrochemical reversibility. The DES shows a wide potential window, which suggests its suitability for high-voltage applications. Based on the experimental evaluations, it can be concluded that the optimum TBAB to oxalic acid ratio for DES formation is 1 : 4. This study explored for the first time the use of a deep eutectic solvent based on oxalic acid and ammonium to optimize and achieve esterification efficiency of 96.3% within 10 min. Greenness analysis by three different methods clearly showed the greenness of the DES-based method over the sulphuric acid-based method.

Conflicts of interest

There are conflicts of interest to declare.

Data availability

All the data have been included in this article.

References

1 J. Gorke, F. Srienc and R. Kazlauskas, *Biotechnol. Bioprocess Eng.*, 2010, **15**, 40–53, DOI: 10.1007/s12257-009-3079-z.
2 L. P. Silva, M. A. R. Martins, D. O. Abranches, S. P. Pinho and J. A. P. Coutinho, *J. Mol. Liq.*, 2021, **337**, 116392, DOI: 10.1016/j.molliq.2021.116392.
3 A. P. Abbott, G. Capper, D. L. Davies, R. K. Rasheed and V. Tambyrajah, *Chem. Commun.*, 2003, **1**, 70–71, DOI: 10.1039/B210714G.
4 Q. Zhang, K. De Oliveira Vigier, S. Royer and F. Jérôme, *Chem. Soc. Rev.*, 2012, **41**, 7108–7146, DOI: 10.1039/C2CS35178A.
5 Y. Ma, *et al.*, *Phytochem. Anal.*, 2018, **29**, 639–648, DOI: 10.1002/pca.2777.
6 H.-G. Liao, Y.-X. Jiang, Z.-Y. Zhou, S.-P. Chen and S.-G. Sun, *Angew. Chem., Int. Ed.*, 2008, **47**, 9100–9103, DOI: 10.1002/anie.200803202.
7 Z. Maugeri and P. María, *RSC Adv.*, 2011, **2**, 421–425, DOI: 10.1039/C1RA00630D.
8 M. Francisco, A. van den Bruinhorst, L. F. Zubeir, C. J. Peters and M. C. Kroon, *Fluid Phase Equilib.*, 2013, **340**, 77–84, DOI: 10.1016/j.fluid.2012.12.001.
9 X. Li, M. Hou, B. Han, X. Wang and L. Zou, *J. Chem. Eng. Data*, 2008, **53**, 1765–1770, DOI: 10.1021/je700638u.
10 M. Venu Chary, N. Keerthysri, S. Vupallapati, N. Lingaiah and S. Kantevari, *Catal. Commun.*, 2008, **9**, 2013–2017, DOI: 10.1016/j.catcom.2008.03.037.
11 M. Mohan, P. K. Naik, T. Banerjee, V. V. Goud and S. Paul, *Fluid Phase Equilib.*, 2017, **448**, 168–177, DOI: 10.1016/j.fluid.2017.05.024.
12 R. Harris, Physical properties of alcohol based deep eutectic solvents, PhD thesis, University of Leicester England, 2009.
13 R. Yusof, K. Jumbri and M. B. A. Rahman, *J. Mol. Liq.*, 2021, **339**, 116709, DOI: 10.1016/j.molliq.2021.116709.
14 F. S. Mjalli, J. Naser, B. Jibril, V. Alizadeh and Z. Gano, *J. Chem. Eng. Data*, 2014, **59**, 2242–2251, DOI: 10.1021/je5002126.
15 S. L. Perkins, P. Painter and C. M. Colina, *J. Chem. Eng. Data*, 2014, **59**, 3652–3662, DOI: 10.1021/je500520h.
16 J. Lilja, D. Yu, D. Murzin, T. Salmi, J. Aumo, P. Mäki-Arvela and M. Sundell, *J. Mol. Catal. A: Chem.*, 2002, **182**, 555–563.
17 L. H. Keith, L. U. Gron and J. L. Young, *Chem. Rev.*, 2007, **107**, 2695–2708, DOI: 10.1021/CR068359E.
18 J. Płotka-Wasylka, *Talanta*, 2018, **181**, 204–209, DOI: 10.1016/j.talanta.2018.01.013.
19 K. Van Aken, L. Strekowski and L. Patiny, *Beilstein J. Org. Chem.*, 2006, **2**(1), 3.
20 J. Li, H. Xiao, X. Tang and M. Zhou, *Energy Fuels*, 2016, **30**, 5411–5418, DOI: 10.1021/acs.energyfuels.6b00471.
21 M. Hayyan, F. S. Mjalli, M. A. Hashim, I. M. AlNashef and T. X. Mei, *J. Ind. Eng. Chem.*, 2013, **19**, 106–112, DOI: 10.1016/j.jiec.2012.07.011.
22 Y. A. T. H. Yeow, A. Hayyan, M. U. M. Junaidi, M. Z. M. Salleh, Y. M. Alanazi, J. Saleh, *et al.*, *J. Ind. Eng. Chem.*, 2024, **140**, 298–310, DOI: 10.1016/j.jiec.2024.05.049.
23 L. Lomba, M. P. Ribate, E. Sangüesa, J. Concha, M. P. Garralaga, D. Errazquin, *et al.*, *Appl. Sci.*, 2021, **11**, 10061, DOI: 10.3390/app112110061.
24 A. Shishov, P. Makoś-Chełstowska, A. Bulatov and V. Andruch, *J. Phys. Chem. B*, 2022, **126**, 21, DOI: 10.1021/acs.jpcb.2c00858.
25 M. Hayyan, F. S. Mjalli, M. A. Hashim, I. M. AlNashef and T. X. Mei, *J. Ind. Eng. Chem.*, 2013, **19**, 106–112, DOI: 10.1016/j.jiec.2012.07.011.
26 R. Pauliukaite, A. P. Doherty, K. D. Murnaghan and C. M. A. Brett, *Electroanalysis*, 2008, **20**, 485–490, DOI: 10.1002/elan.200704081.
27 M. A. Brett, *Curr. Opin. Electrochem.*, 2018, **10**, 143–148, DOI: 10.1016/j.coelec.2018.05.016.

28 A. P. Abbott, D. Boothby, G. Capper, D. L. Davies and R. K. Rasheed, *J. Am. Chem. Soc.*, 2004, **126**, 9142–9147, DOI: 10.1021/ja048266j.
29 H. Zhao, G. A. Baker and S. Holmes, *Org. Biomol. Chem.*, 2011, **9**, 1908–1916, DOI: 10.1039/C0OB01011A.
30 A. L. Sazali, N. AlMasoud, S. K. Amran, T. S. Alomar, K. F. Pa'ee, Z. M. El-Bahy, T. L. K. Yong, D. J. Dailin and L. F. Chuah, *Chemosphere*, 2023, **338**, 139485, DOI: 10.1016/j.chemosphere.2023.139485.
31 A. P. Abbott, R. C. Harris, K. S. Ryder, C. D'Agostino, L. F. Gladden and M. D. Mantle, *Green Chem.*, 2011, **13**, 82–90, DOI: 10.1039/C0GC00395F.
32 D. Yue, Y. Jing, J. Ma, Y. Yao and Y. Jia, *J. Therm. Anal. Calorim.*, 2012, **110**, 773–780, DOI: 10.1007/s10973-011-1960-4.
33 A. N. Siyal, S. Q. Memon and M. I. Khaskheli, *Pol. J. Chem. Technol.*, 2012, **14**(1), 71–77.
34 F. Aisha and I. Zahrina, *Mater. Today: Proc.*, 2023, **87**, 303–310, DOI: 10.1016/j.matpr.2023.03.286.
35 A. Abdurrahman, S. Waziri, O. Ajayi and F. Dabai, *J. Niger. Soc. Phys. Sci.*, 2023, **5**, 1048, DOI: 10.46481/jnsps.2023.1048.
36 S. Listiana, *et al.*, *IOP Conf. Ser. Earth Environ. Sci.*, 2023, **1201**, 012099, DOI: 10.1088/1755-1315/1201/1/012099.
37 S. T. Williamson, K. Shahbaz, F. S. Mjalli, I. M. AlNashef and M. M. Farid, *Renewable Energy*, 2017, **114**, 480–488, DOI: 10.1016/j.renene.2017.07.046.
38 D. Rahmi and N. Neswati, *Int. J. Adv. Sci. Eng. Inf. Technol.*, 2013, **3**, 338–342.
39 V. Russo, *et al.*, *Chem. Eng. J.*, 2021, **408**, 127236, DOI: 10.1016/j.cej.2020.127236.
40 N. Al-Arafi and J. Salimon, *J. Chem.*, 2012, **9**, 181249, DOI: 10.1155/2012/181249.
41 C. C. A. Loures, M. S. Amaral, P. C. M. D. Rós, S. M. F. E. Zorn, H. F. de Castro and M. B. Silva, *Fuel*, 2018, **211**, 261–268, DOI: 10.1016/j.fuel.2017.09.073.
42 G. Lawer-Yolar, B. Dawson-Andoh and E. Atta-Obeng, *Sustainable Chem.*, 2021, **2**, 206–221, DOI: 10.3390/suschem2010012.
43 U.S. Environmental Protection Agency. Emergency Planning and Community Right-to-Know Act; Section 313; Toxic Release Inventory (TRI). 2006. available at: http://www.epa.gov/tri/chemical/.
44 U.S. Government. Code of Federal Regulations, Title 40, Part 261. 2006. available at: http://ecfr.gpoaccess.gov.
45 A. Gałuszka, Z. M. Migaszewski, P. Konieczka and J. Namieśnik, *TrAC, Trends Anal. Chem.*, 2012, **37**, 61–72.
46 Y. M. Park, J. Y. Lee, S. H. Chung, I. S. Park, S. Y. Lee, D. K. Kim and K. Y. Lee, *Bioresour. Technol.*, 2010, **101**, S59–S61, DOI: 10.1016/j.biortech.2009.04.025.
47 F. Mirshafiee and M. Rezaei, *J. Mol. Liq.*, 2025, **426**, 127333, DOI: 10.1016/j.molliq.2025.127333.
48 S. Hou and W. Xie, *Renewable Energy*, 2025, **250**, DOI: 10.1016/j.renene.2025.123303.
49 P. Mardina, H. Wijayanti, R. Juwita, M. D. Putra, I. F. Nata, R. Lestari and L. Lestari, *Indones. J. Sci. Technol.*, 2024, **9**(1), 109–124.
50 M. G. Mustafa, B. Singh, G. P. Singh and R. K. Dey, *Sustain. Chem. One World*, 2025, **5**, 100034, DOI: 10.1016/j.scowo.2024.100034.
51 H. Zhang, *et al.*, *Carbon*, 2019, **147**, 134–145, DOI: 10.1016/j.carbon.2019.02.079.
52 M. Ayadi, S. Awad, A. Villot, M. Abderrabba and M. Tazerout, *Renewable Energy*, 2021, **165**, 1–13, DOI: 10.1016/j.renene.2020.11.031.
53 A. Hayyan, *et al.*, *J. Mol. Liq.*, 2021, **344**, 117574, DOI: 10.1016/j.molliq.2021.117574.
54 Y. Li, *et al.*, *Fuel Process. Technol.*, 2023, **239**, 107558, DOI: 10.1016/j.fuproc.2022.107558.
55 J. Zhu, W. Jiang, Z. Yuan, J. Lu and J. Ding, *Renewable Energy*, 2024, **221**, 119760, DOI: 10.1016/j.renene.2023.119760.